Full-Duplex Enabled Cloud Radio Access Network

Arman Shojaeifard*, Kai-Kit Wong*, Wei Yu†, Gan Zheng‡, and Jie Tang§
*Electronic and Electrical Engineering Department, University College London, London, United Kingdom
†Electrical and Computer Engineering Department, University of Toronto, Toronto, Ontario, Canada
‡Mechanical, Electrical and Manufacturing Engineering, Loughborough University, Loughborough, United Kingdom
§School of Electronic and Information Engineering, South China University of Technology, Guangzhou, China
*a.shojaeifard@ucl.ac.uk; *kai-kit.wong@ucl.ac.uk; †weiyu@ece.utoronto.ca; ‡g.zheng@lboro.ac.uk; §eejtang@scut.edu.cn.

***Abstract*—Full-duplex (FD) has emerged as a disruptive solution for improving the achievable spectral efficiency (SE), thanks to the recent major breakthroughs in self-interference (SI) mitigation. The FD versus half-duplex (HD) SE gain, in the context of cellular networks, is however largely limited by the mutual interference (MI) between the downlink (DL) and uplink (UL). A potential remedy for tackling the MI bottleneck is through cooperative communications. This paper provides a stochastic analysis of FD enabled cloud radio access network (C-RAN) with finite user-centric cooperative clusters. Contrary to the most existing theoretical studies of C-RAN, we explicitly take into consideration non-isotropic fading channel conditions, and finite-capacity fronthaul links. Accordingly, we develop analytical expressions for the FD C-RAN DL and UL SEs. The results indicate that significant FD versus HD C-RAN SE gains can be achieved, particularly in the presence of sufficient-capacity fronthaul links and advanced interference cancellation capabilities.**

I. Introduction

Cloud radio access network (C-RAN) is a novel cellular system architecture, intended to tackle the various underlying challenges posed by network densification [1], [2]. C-RAN facilitates cooperative communications on a large-scale basis [3], with central processors (CPs) handling the baseband processing and, via fronthaul links, exchanging information with distributed radio units (RUs), which in turn, provide (mostly) radio-frequency functionalities. C-RAN, thanks to its ability to address the inter-cell interference phenomenon, can provide significantly higher spectral efficiency (SE) and energy efficiency (EE) versus the legacy cellular systems [4], [5].

Another emerging disruptive solution for improving the data rates is full-duplex (FD) communications, that is transceiving of information at the same time and frequency [6]. This trend follows from the recent major breakthroughs in signal processing techniques which combat self-interference (SI) directly in FD mode [7], [8]. On the other hand, the FD versus half-duplex (HD) SE gain, in cellular networks, is largely limited by the mutual interference (MI) between the downlink (DL) and uplink (UL) [9]–[11]. A potential remedy for tackling the MI bottleneck is through cooperative communications, also referred to as network multiple-input multiple-output (MIMO).

In [12], the performance of C-RAN with FD enabled RUs was studied using the classical Wyner cellular model. In particular, the authors derived analytical expressions for the C-RAN DL and UL SEs in both FD and HD modes of communications. In [13], a FD multi-cell network MIMO scenario was considered. By utilizing spatial interference-alignment (IA), the authors derived the FD versus HD scaling multiplexing gain in closed-form. Moreover, the performance of C-RAN with a single FD user equipment (UE) and randomly-deployed HD multi-antenna RUs was investigated under different beamforming and RU association schemes in [14].

In this work, we provide a stochastic analysis of large-scale C-RAN with FD enabled multi-antenna RUs (relays). Here, the finite clusters in the C-RAN are formed dynamically in a user-centric manner. We explicitly take into account the inherent non-isotropic fading conditions, and utilize the Gamma moment-matching technique to characterize the different signals power distributions. The impact of capacity-limited fronthaul links is included in the analysis using cut-set bounds on the achievable SE. Accordingly, we develop analytical expressions for the DL and UL SEs in the FD C-RAN under consideration. The validity of the proposed theoretical framework is confirmed through Monte-Carlo (MC) simulations. The results highlight the promising potential of FD versus HD operation with regards to the C-RAN achievable SE, particularly, in the presence of sufficient-capacity fronthaul links and advanced interference cancellation capabilities.

Notation. $\boldsymbol{X}$ is a matrix; $\boldsymbol{x}$ is a vector; T, $\dagger$, and $+$ represent the transpose, Hermitian, and pseudo-inverse; j is the imaginary unit; $\mathrm{Im}(.)$ is the imaginary part; $\mathbb{E}[.]$ is the expectation; $\mathscr{P}[.]$ is the probability; $\mathcal{F}_x[.]$ is the cumulative distribution function (CDF); $\mathcal{P}_x[.]$ is the probability density function (PDF); $\mathcal{M}[.]$ is the moment-generating-function (MGF); $|x|$ is the modulus; $\|\boldsymbol{x}\|$ is the Euclidean norm; $\mathbf{I}_{(.)}$ is the identity matrix; Null(.) is a nullspace; $\mathcal{CN}(\mu,\nu^2)$ is the circularly-symmetric complex Gaussian distribution with mean μ and variance ν^2; $\Gamma(.)$ and $\Gamma(.,.)$ are the Gamma and incomplete (upper) Gamma functions; $\mathcal{G}(\kappa,\theta)$ is the Gamma distribution with shape parameter κ and scale parameter θ; and ${}_2F_1(.,.;.;.)$ is the Gauss hypergeometric function, respectively.

II. C-RAN Description

Consider a large-scale C-RAN in which the multi-antenna RUs and UEs follow from independent Poisson point processes (PPPs) $\Phi^{(d)}$ and $\Phi^{(u)}$ with densities $\lambda^{(d)}$ and $\lambda^{(u)}$, respectively. Here, we consider the user-centric approach towards forming of the finite clusters in the C-RAN. Within any cluster, a CP is considered to facilitate cooperative communications between the multi-antenna RUs and UEs. In the FD enabled C-RAN, each RU, equipped with $N^{(d)}$ transmit and $N^{(u)}$ receive

antennas, is considered to be serving $\mathcal{K}^{(d)}$ ($\leq N^{(d)}$) HD DL UEs and $\mathcal{K}^{(u)}$ ($\leq N^{(u)}$) HD UL UEs, all equipped with single antennas, per resource block [15]. The transmit powers of the multi-antenna RUs and UEs are denoted with $p^{(d)}$ (per-user) and $p^{(u)}$, respectively. We utilize the Rayleigh distribution to model the small-scale fading channels. The distance-dependent path-loss model with exponent α is employed, i.e., $\beta_{a,b} = r_{a,b}^{-\alpha}$, where $r_{a,b}$ is the Euclidean distance between a and b. The number of RUs in a cluster c is denoted with L_c. The impact of residual SI is considered to be negligible compared to the MI [12]. We take into account successive interference cancellation (SIC) at the UE side by imposing a guard region of arbitrary radius in the respective MI expression.

Here, we use $\boldsymbol{g}_{m_l,c_k} = \sqrt{\beta_{m_l,c_k}}\boldsymbol{f}_{m_l,c_k}$, where $\boldsymbol{f}^T_{m_l,c_k} \sim \mathcal{CN}(\mathbf{0}, \mathbf{I}_{N^{(d)}})$, in order to denote the DL channel from the RU l in the cluster m to the UE k in the cluster c. The combined DL channel from the L_m RUs in the cluster m to the UE k in the cluster c is represented using $\boldsymbol{g}_{m,c_k} = [\boldsymbol{g}_{m_l,c_k}]_{1\leq l\leq L_m} \in \mathcal{C}^{1\times L_m N^{(d)}}$. Moreover, $\boldsymbol{h}_{c_k,m_l} = \sqrt{\beta_{c_k,m_l}}\boldsymbol{f}_{c_k,m_l}$, where $\boldsymbol{f}_{c_k,m_l} \sim \mathcal{CN}(\mathbf{0}, \mathbf{I}_{N^{(u)}})$, is used to represent the UL channel from the UE k in the cluster c to the RU l in the cluster m. The combined UL channel to the RUs in the cluster m from the UE k in the cluster c is given by $\boldsymbol{h}_{c_k,m} = [\boldsymbol{h}^T_{c_k,m_l}]^T_{1\leq l\leq L_m} \in \mathcal{C}^{L_m N^{(u)}\times 1}$. The cross-mode channel from the UL UE k in the cluster m to the DL UE o in the cluster c is denoted with $h_{m_k,c_o} = \sqrt{\beta_{m_k,c_o}} f_{m_k,c_o}$, where $f_{m_k,c_o} \sim \mathcal{CN}(0,1)$. The cross-mode channel from the RU l in the cluster m to the RU b in the cluster c is given by $\boldsymbol{G}_{m_l,c_b} = \sqrt{\beta_{m_l,c_b}}\boldsymbol{F}_{m_l,c_b}$, where $\boldsymbol{F}_{m_l,c_b} \sim \mathcal{CN}(\mathbf{0}, \mathbf{I}_{N^{(u)}\times N^{(d)}})$. We can then express the channel from the RU l in the cluster m to the RUs in the cluster c using $\boldsymbol{G}_{m_l,c} = [\boldsymbol{G}^T_{m_l,c_b}]^T_{0\leq b\leq L_c} \in \mathcal{C}^{L_c N^{(u)}\times N^{(d)}}$. In addition, we accordingly represent the channel from the RUs in the cluster m to the RUs in the cluster c using $\boldsymbol{G}_{m,c} = [\boldsymbol{G}_{m_l,c}]_{1\leq l\leq L_m} \in \mathcal{C}^{L_c N^{(u)}\times L_m N^{(d)}}$.

Let $\boldsymbol{G}_c = [\boldsymbol{g}^T_{c,c_k}]^T_{1\leq k\leq L_c\mathcal{K}^{(d)}} \in \mathcal{C}^{L_c\mathcal{K}^{(d)}\times L_c N^{(d)}}$ denote the combined DL channel from the RUs to the DL UEs in the cluster c. Moreover, $\boldsymbol{s}_c = [s_{c,c_k}]^T_{1\leq k\leq L_c\mathcal{K}^{(d)}} \in \mathcal{C}^{L_c\mathcal{K}^{(d)}\times 1}$, $\mathbb{E}\left\{|s_{c,c_k}|^2\right\} = 1$, is the DL complex symbol vector from the RUs to the DL UEs in the cluster c. The normalized linear precoding matrix at the cluster c is $\boldsymbol{V}_c = [\boldsymbol{v}_{c,c_k}]_{1\leq k\leq L_c\mathcal{K}^{(d)}} \in \mathcal{C}^{L_c N_t\times L_c\mathcal{K}^{(d)}}$, $\mathbb{E}\{\|\boldsymbol{v}_{c,c_k}\|^2\} = 1$. The DL received signal for the reference DL UE c_o in the cluster c is given by (1) where Ψ is the set of all clusters, $\Psi^{(d)}_c$ is the set of DL UEs in the cluster c, $\Psi^{(u)}_m$ is the set of UL UEs in the cluster m, $s_{m_k,m}$ is the information symbol transmitted from the UL UE k in the cluster m, and $\eta^{(d)}$ is the zero-mean complex additive white Gaussian noise (AWGN) with variance $\nu^{(d)}$, respectively. Further, let $\boldsymbol{H}_c = [\boldsymbol{h}_{c_k,c}]_{1\leq k\leq L_c\mathcal{K}^{(u)}} \in \mathcal{C}^{L_c N^{(u)}\times L_c\mathcal{K}^{(u)}}$ denote the combined UL channel from the UL UEs at the RUs in the cluster c. The normalized linear postcoding matrix at the CP in the cluster c is $\boldsymbol{W}_c = [\boldsymbol{w}^T_{c_k,c}]^T_{1\leq k\leq L_c\mathcal{K}^{(u)}} \in \mathcal{C}^{L_c\mathcal{K}^{(u)}\times L_c N^{(u)}}$, $\mathbb{E}\{\|\boldsymbol{w}_{c_k,c}\|^2\} = 1$. The UL received signal from the reference UL UE c_i in the cluster c is given by (2) where $\boldsymbol{\eta}^{(u)} \in \mathcal{C}^{L_c N^{(u)}\times 1}$ is the circularly-symmetric zero-mean complex AWGN vector with covariance matrix $\nu^{(u)}\mathbf{I}_{L_c N^{(u)}}$.

III. Signals Distributions

In the DL, the CP, in each cluster, carries out the baseband processing, and forwards the corresponding information via fronthaul links to the RUs. Here, we adopt a linear ZF precoder for suppressing intra-cluster interference in the DL. In the cluster c, $\boldsymbol{V}_c$ is set equal to the normalized columns of $\boldsymbol{G}^+_c = \boldsymbol{G}^\dagger_c(\boldsymbol{G}_c\boldsymbol{G}^\dagger_c)^{-1} \in \mathcal{C}^{L_c N^{(d)}\times L_c\mathcal{K}^{(d)}}$. In the UL, the signals received at the RUs from the UL UEs are compressed, and forwarded via fronthaul links to the CP. The CP, in turn, performs joint decoding. Here, we adopt a linear ZF postcoder for suppressing intra-cluster interference in the UL. In the cluster c, the normalized rows of $\boldsymbol{H}^+_c = (\boldsymbol{H}^\dagger_c\boldsymbol{H}_c)^{-1}\boldsymbol{H}^\dagger_c \in \mathcal{C}^{L_c\mathcal{K}^{(d)}\times L_c N^{(u)}}$ are set equal to the row vectors of $\boldsymbol{W}_c$.

We proceed by defining the signal-to-interference-plus-noise ratios (SINRs) in the FD C-RAN under consideration. The received SINR at the reference DL UE o in the cluster c is given by

$$\gamma^{(d)} = \frac{\mathcal{X}^{(d)}}{\mathcal{CI}^{(d)} + \mathcal{MI}^{(d)} + \nu^{(d)}} \tag{3}$$

where $\mathcal{X}^{(d)} = p^{(d)}|\boldsymbol{g}_{c,c_o}\boldsymbol{v}_{c,c_o}|^2$, $\mathcal{CI}^{(d)} = p^{(d)}\sum_{m\in\Psi}\|\boldsymbol{g}_{m,c_o}\boldsymbol{V}_m\|^2$, and $\mathcal{MI}^{(d)} = p^{(u)}\sum_{m\in\Psi, m_k\in\Psi^{(u)}_m}|h_{m_k,c_o}|^2$. Further, in the cluster c, the received SINR for the reference UL UE i at the CP is given by

$$\gamma^{(u)} = \frac{\mathcal{X}^{(u)}}{\mathcal{CI}^{(u)} + \mathcal{MI}^{(u)} + \nu^{(u)}} \tag{4}$$

where $\mathcal{X}^{(u)} = p^{(u)}|\boldsymbol{w}^T_{c_i,c}\boldsymbol{h}_{c_i,c}|^2$, $\mathcal{CI}^{(u)} = p^{(u)}\sum_{m\in\Psi\setminus\{c\}, m_k\in\Psi^{(u)}_m}|\boldsymbol{w}^T_{c_i,c}\boldsymbol{h}_{m_k,c}|^2$, and $\mathcal{MI}^{(u)} = p^{(d)}\sum_{m\in\Psi\setminus\{c\}}\|\boldsymbol{w}^T_{c_i,c}\boldsymbol{G}_{m,c}\boldsymbol{V}_m\|^2$.

In the case of cooperative communications, for example in the C-RAN, the channels are non-isotropic in nature [16], given that the links between randomly-located RUs and UEs involve different distance-dependent path-loss parameters. As a result, it is not possible to derive the exact distributions of the different useful and interference channel power gains. In what follows, we apply the Gamma moment matching technique to characterize the different channel power gains in the context of FD C-RAN with finite user-centric cooperative clusters. Note that the average number of RUs per cluster is denoted with L.

Approximation 1. The DL and UL useful channel power gains with linear ZF beamforming in the FD C-RAN under consideration are respectively given by

$$|\boldsymbol{g}_{c,c_o}\boldsymbol{v}_{c,c_o}|^2 \approx \sum_{c_j\in\Phi^{(d)}_c}\beta_{c_j,c_o}\psi_{c_j,c_o},$$
$$\psi_{c_j,c_o} \sim \mathcal{G}\left(N^{(d)} - \mathcal{K}^{(d)} + \frac{1}{L}, 1\right) \tag{5}$$

$$\left|\boldsymbol{w}^T_{c_i,c}\boldsymbol{h}_{c_i,c}\right|^2 \approx \sum_{c_l\in\Phi^{(d)}_c}\beta_{c_i,c_l}\psi_{c_i,c_l},$$
$$\psi_{c_i,c_l} \sim \mathcal{G}\left(N^{(u)} - \mathcal{K}^{(u)} + \frac{1}{L}, 1\right). \tag{6}$$

$$y^{(d)} = \underbrace{\sqrt{p^{(d)}}\boldsymbol{g}_{c,c_o}\boldsymbol{v}_{c,c_o}s_{c,c_o}}_{\text{useful signal}} + \underbrace{\sqrt{p^{(d)}}\boldsymbol{g}_{c,c_o}\sum_{c_k\in\Psi_c^{(d)}\setminus\{c_o\}}\boldsymbol{v}_{c,c_k}s_{c,c_k}}_{\text{intra-cluster interference}} + \underbrace{\sqrt{p^{(d)}}\sum_{m\in\Psi\setminus\{c\}}\boldsymbol{g}_{m,c_o}\boldsymbol{V}_m\boldsymbol{s}_m}_{\text{inter-cluster interference}}$$
$$+ \underbrace{\sqrt{p^{(u)}}\sum_{m\in\Psi,m_k\in\Psi_m^{(u)}}h_{m_k,c_o}s_{m_k,m}}_{\text{mutual interference}} + \underbrace{\eta^{(d)}}_{\text{noise}} \tag{1}$$

$$y^{(u)} = \underbrace{\sqrt{p^{(u)}}\boldsymbol{w}_{c_i,c}^T\boldsymbol{h}_{c_i,c}s_{c_i,c}}_{\text{useful signal}} + \underbrace{\sqrt{p^{(u)}}\sum_{c_k\in\Psi_c^{(u)}\setminus\{c_i\}}\boldsymbol{w}_{c_i,c}^T\boldsymbol{h}_{c_k,c}s_{c_k,c}}_{\text{intra-cluster interference}} + \underbrace{\sqrt{p^{(u)}}\sum_{m\in\Psi\setminus\{c\},m_k\in\Psi_m^{(u)}}\boldsymbol{w}_{c_i,c}^T\boldsymbol{h}_{m_k,c}s_{m_k,m}}_{\text{inter-cluster interference}}$$
$$+ \underbrace{\sqrt{p^{(d)}}\sum_{m\in\Psi\setminus\{c\}}\boldsymbol{w}_{c_i,c}^T\boldsymbol{G}_{m,c}\boldsymbol{V}_m\boldsymbol{s}_m}_{\text{mutual interference}} + \underbrace{\boldsymbol{w}_{c_0,c}^T\boldsymbol{\eta}^{(u)}}_{\text{scaled noise}} \tag{2}$$

Approximation 2. The DL and UL inter-cluster interference channel power gains with linear ZF beamforming in the FD C-RAN under consideration are respectively given by

$$\|\boldsymbol{g}_{m,c_o}\boldsymbol{V}_m\|^2 \approx \sum_{m_j\in\Phi_m^{(d)}}\beta_{m_j,c_o}\psi_{m_j,c_o}, \quad \psi_{m_j,c_o}\sim\mathcal{G}\left(\mathcal{K}^{(d)},1\right) \tag{7}$$

$$\left|\boldsymbol{w}_{c_i,c}^T\boldsymbol{h}_{m_k,c}\right|^2 \approx \sum_{c_l\in\Phi_c^{(d)}}\beta_{m_k,c_l}\psi_{m_k,c_l}, \quad \psi_{m_k,c_l}\sim\mathcal{G}\left(\frac{1}{L},1\right). \tag{8}$$

Approximation 3. The DL and UL cross-mode interference channel power gains with linear ZF beamforming in the FD C-RAN under consideration are respectively given by

$$|h_{m_k,c_o}|^2 = \beta_{m_k,c_o}\psi_{m_k,c_o},\ \psi_{m_k,c_o}\sim\mathcal{G}(1,1) \tag{9}$$

$$\left\|\boldsymbol{w}_{c_i,c}^T\boldsymbol{G}_{m,c}\boldsymbol{V}_m\right\|^2 \approx \sum_{m_j\in\Phi_m^{(d)}}\sum_{c_l\in\Phi_c^{(d)}}\beta_{m_j,c_l}\psi_{m_j,c_l}, \quad \psi_{m_j,c_l}\sim\mathcal{G}\left(\frac{\mathcal{K}^{(d)}}{L},1\right). \tag{10}$$

Proof: Omitted due to the space limitations.

IV. Spectral Efficiency Analysis

In the C-RAN, the achievable SE under finite-capacity fronthaul links is upper-bounded with respect to the information-theoretic cut-set bound [17]. We consider the normalized per-user DL and UL capacities of the fronthaul links are $C^{(d)}$ and $C^{(u)}$ (in nat/s/Hz), respectively [12]. Note that $\log\left(1+\gamma^{(d)}\right)$ and $\log\left(1+\gamma^{(u)}\right)$ respectively denote the C-RAN instantaneous DL and UL per-user SEs (in nat/s/Hz). Hence, we can characterize the C-RAN bounded DL and UL SEs in the presence of capacity-limited fronthaul links.

Theorem 1. In the FD C-RAN under capacity-limited fronthaul links, the achievable per-user DL and UL SEs (in nat/s/Hz) can be respectively upper-bounded by the cut-set bound theorem as

$$\mathcal{S}^{(d)} \le \mathbb{E}\left[\min\left(\log\left(1+\gamma^{(d)}\right),C^{(d)}\right)\right] = \int_0^{C^{(d)}}\frac{1}{1+x}\left(1-\mathcal{F}_{\gamma^{(d)}}[x]\right)\mathrm{d}x \tag{11}$$

$$\mathcal{S}^{(u)} \le \mathbb{E}\left[\min\left(\log\left(1+\gamma^{(u)}\right),C^{(u)}\right)\right] = \int_0^{C^{(u)}}\frac{1}{1+x}\left(1-\mathcal{F}_{\gamma^{(u)}}[x]\right)\mathrm{d}x. \tag{12}$$

Proof: Omitted due to the space limitations.

Next, we adopt the Gil-Pelaez theorem [18] to derive, for the first time, explicit expressions for the FD C-RAN DL and UL coverage probabilities over non-isotropic fading channels.

Theorem 2. The CDFs of the DL and UL SINRs in the FD C-RAN under consideration are respectively given by

$$\mathcal{F}_{\gamma^{(d)}}[x] = \frac{1}{2} - \frac{1}{\pi}\int_0^\infty\frac{1}{s}\,\mathrm{Im}\left(\mathcal{M}_{\Theta^{(d)}}[js]\exp\left(js\nu^{(d)}\right)\right)\mathrm{d}s \tag{13}$$

$$\mathcal{F}_{\gamma^{(u)}}[x] = \frac{1}{2} - \frac{1}{\pi}\int_0^\infty\frac{1}{s}\,\mathrm{Im}\left(\mathcal{M}_{\Theta^{(u)}}[js]\exp\left(js\nu^{(u)}\right)\right)\mathrm{d}s \tag{14}$$

where

$$\mathcal{M}_{\Theta^{(d)}}[js] = \mathcal{M}_{\mathcal{CI}^{(d)}}[js]\,\mathcal{M}_{\mathcal{MI}^{(d)}}[js]\,\mathcal{M}_{\mathcal{X}^{(d)}}\left[\frac{-js}{x}\right] \tag{15}$$

$$\mathcal{M}_{\Theta^{(u)}}[js] = \mathcal{M}_{\mathcal{CI}^{(u)}}[js]\,\mathcal{M}_{\mathcal{MI}^{(u)}}[js]\,\mathcal{M}_{\mathcal{X}^{(u)}}\left[\frac{-js}{x}\right]. \tag{16}$$

Proof: Omitted due to the space limitations.

Next, we need to characterize the statistics of the different useful and interference signals. We proceed by defining the following functions which are used in the analysis

$$\Xi(y,\theta,\mathcal{R}) \triangleq \sqrt{\mathcal{R}^2 - y^2\cos^2(\theta)} + y\sin(\theta) \tag{17}$$

$$\begin{aligned}\mathscr{F}_1(z,p,\alpha,\mathcal{P},\mathcal{Q},T) &\triangleq \int_0^T \left(1-\left(1+zpr^{-\alpha}\mathcal{Q}\right)^{-\mathcal{P}}\right) r\ \mathrm{d}r \\ &= \frac{1}{2}T^2\Bigg(1-\frac{2}{\alpha\mathcal{P}+2}\left(\frac{T^\alpha}{zp\mathcal{Q}}\right)^{\mathcal{P}}\times \\ &\quad {}_2F_1\left(\mathcal{P},\mathcal{P}+\frac{2}{\alpha};\mathcal{P}+\frac{2}{\alpha}+1;-\frac{T^\alpha}{zp\mathcal{Q}}\right)\Bigg)\end{aligned} \tag{18}$$

$$\begin{aligned}\mathscr{F}_2(z,p,\alpha,\mathcal{P},\mathcal{Q},T) &\triangleq \int_T^\infty \left(1-\left(1+zpr^{-\alpha}\mathcal{Q}\right)^{-\mathcal{P}}\right) r\ \mathrm{d}r \\ &= \frac{1}{2}T^2\left({}_2F_1\left(-\frac{2}{\alpha},\mathcal{P};1-\frac{2}{\alpha};-\frac{zp\mathcal{Q}}{T^\alpha}\right)-1\right).\end{aligned} \tag{19}$$

Theorem 3. The statistics of the different DL and UL useful and interference signals in the FD C-RAN under consideration are given by

$$\begin{aligned}\mathcal{M}_{\mathcal{X}^{(d)}}[js] = \exp\Bigg(&-2\pi\lambda^{(d)}\times \\ &\mathscr{F}_1\left(js,p^{(d)},\alpha,N^{(d)}-\mathcal{K}^{(d)}+\frac{1}{L},1,\mathcal{R}\right)\Bigg)\end{aligned} \tag{20}$$

$$\begin{aligned}\mathcal{M}_{\mathcal{X}^{(u)}}[js] = \exp\Bigg(&-2\pi\lambda^{(d)}\times \\ &\mathscr{F}_1\left(js,p^{(u)},\alpha,N^{(u)}-\mathcal{K}^{(u)}+\frac{1}{L},1,\mathcal{R}\right)\Bigg)\end{aligned} \tag{21}$$

$$\mathcal{M}_{\mathcal{CI}^{(d)}}[js] = \exp\left(-2\pi\lambda^{(d)}\mathscr{F}_2\left(js,p^{(d)},\alpha,\mathcal{K}^{(d)},1,\mathcal{R}\right)\right) \tag{22}$$

$$\begin{aligned}\mathcal{M}_{\mathcal{CI}^{(u)}}[js] = \exp\Bigg(&-2\pi\lambda^{(d)}\int_0^{\mathcal{R}}\Bigg(1-\exp\Bigg(-\lambda^{(u)} \\ &\int_0^{2\pi}\mathscr{F}_2\left(js,p^{(u)},\alpha,\frac{1}{L},1,\Xi(y,\theta,\mathcal{R})\right)\mathrm{d}\theta\Bigg)\Bigg)y\ \mathrm{d}y\Bigg)\end{aligned} \tag{23}$$

$$\mathcal{M}_{\mathcal{MI}^{(d)}}(js) = \exp\left(-2\pi\lambda^{(u)}\mathscr{F}_2\left(js,p^{(u)},\alpha,1,1,\mathcal{E}\right)\right) \tag{24}$$

$$\begin{aligned}\mathcal{M}_{\mathcal{MI}^{(u)}}[js] = \exp\Bigg(&-2\pi\lambda^{(d)}\int_0^{\mathcal{R}}\Bigg(1-\exp\Bigg(-\lambda^{(d)} \\ &\int_0^{2\pi}\mathscr{F}_2\left(js,p^{(d)},\alpha,\frac{\mathcal{K}^{(d)}}{L},1,\Xi(y,\theta,\mathcal{R})\right)\mathrm{d}\theta\Bigg)\Bigg)y\ \mathrm{d}y\Bigg).\end{aligned} \tag{25}$$

Proof: Omitted due to the space limitations.

V. Numerical Results

We provide some numerical examples to draw insights into the performance of FD versus HD C-RAN. The RU deployment density is $\lambda^{(d)} = \frac{4}{\pi}$ per km^2. The total system bandwidth is $W = 10$ MHz. The corresponding noise variance is $\nu^{(d)} = \nu^{(u)} = -174 + 10\log_{10}(W) = -104$ dBm. The DL (per user) and UL transmit powers are 23 dBm and 20 dBm, respectively. The path-loss exponent is $\alpha = 4$. The results of the MC simulations are obtained based on 20000 trials in a circular region of radius 50 km. In the FD C-RAN, the DL and UL occur at the same time and frequency, whereas in the HD C-RAN, the DL and UL are separated in time. To facilitate comparison, we consider the per-user SE performance over two resource blocks. All FD results correspond to the case with SIC (at the UE side) and SI cancellation (at the BS side).

1) Impact of Cooperation: We investigate the impact of cooperation on the FD and HD C-RAN SEs in Fig. 1. In the DL, the SE always improves with larger cluster size (L), and furthermore, the FD over HD C-RAN DL SE gain increases in L. A similar trend holds in the UL, where the SEs of the HD and FD C-RANs improve as L is increased. The FD over HD C-RAN UL SE gain is also enhanced in L. The highest FD versus HD C-RAN DL and UL SE gains recorded here are 86.4% and 45.1% (with $L = 8$), respectively. Note that the MC results confirm the validity of the theoretical findings.

2) Impact of the Number of Antennas: Next, we study the FD and HD C-RAN SE performances under different number of RU transmit/receive antennas. We can observe, based on the results from Fig. 2, that by increasing $N^{(d)}$ and $N^{(u)}$, higher DL and UL SEs can be achieved, respectively. Furthermore, the FD over HD SE gain in both DL and UL increases logarithmically in the number of antennas at the RUs.

3) Impact of Fronthaul: Finally, we study the impact of capacity-limited fronthaul on the FD and HD C-RAN SEs in Fig. 3. As expected, increasing the fronthaul capacity enhances the C-RAN SE performance. Furthermore, the FD over HD C-RAN SE gain in both DL and UL increases with greater fronthaul capacity. The fronthaul SE in practice is anticipated to be one or more orders of magnitude greater than the DL or the UL SE [12]. The results from Fig. 3 illustrate that in such cases the FD and HD SEs converge, hence, with sufficient-capacity fronthaul links, significant SE gains can be achieved through FD enabled RUs.

VI. Conclusions

This paper provided a stochastic analysis for large-scale FD enabled C-RAN with finite user-centric cooperative clusters. We incorporated the notion of non-isotropic wireless channels in characterizing the signals power distributions. Explicit spectral efficiency expressions were accordingly derived considering finite-capacity fronthaul links. The results indicated that the FD over HD SE gain can be enhanced considerably through exploiting the cooperative communications capabilities of C-RAN. The respective improvement in SE was particularly evident under sufficient-capacity fronthaul links and advanced interference cancellation solutions.

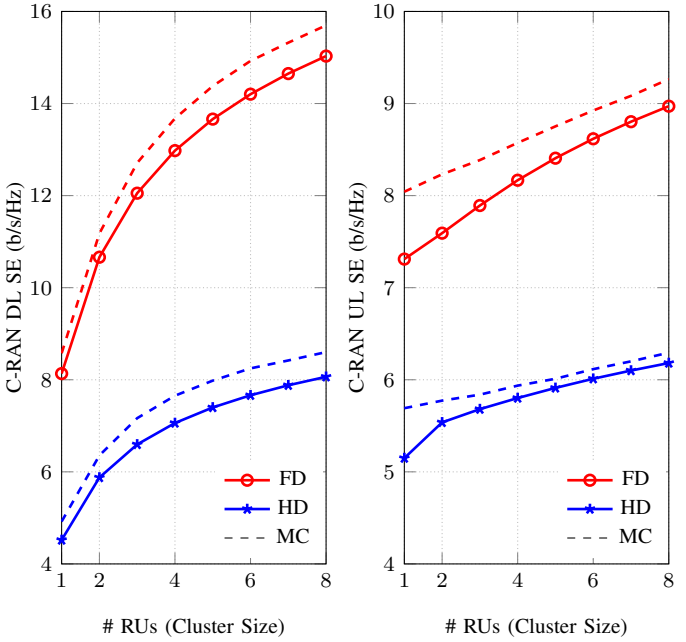

Fig. 1: $N^{(d)} = N^{(u)} = 8$, $\mathcal{K}^{(d)} = \mathcal{K}^{(u)} = 1$.

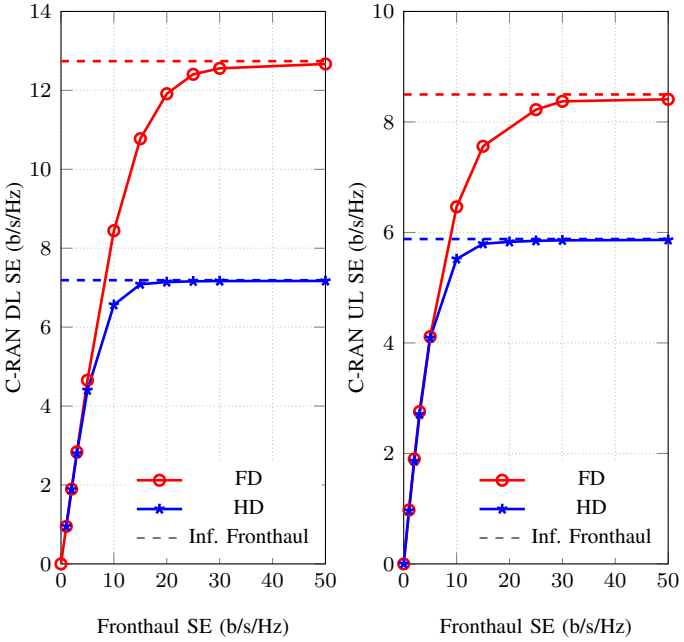

Fig. 3: $L = 3$, $N^{(d)} = N^{(u)} = 8$, $\mathcal{K}^{(d)} = \mathcal{K}^{(u)} = 1$.

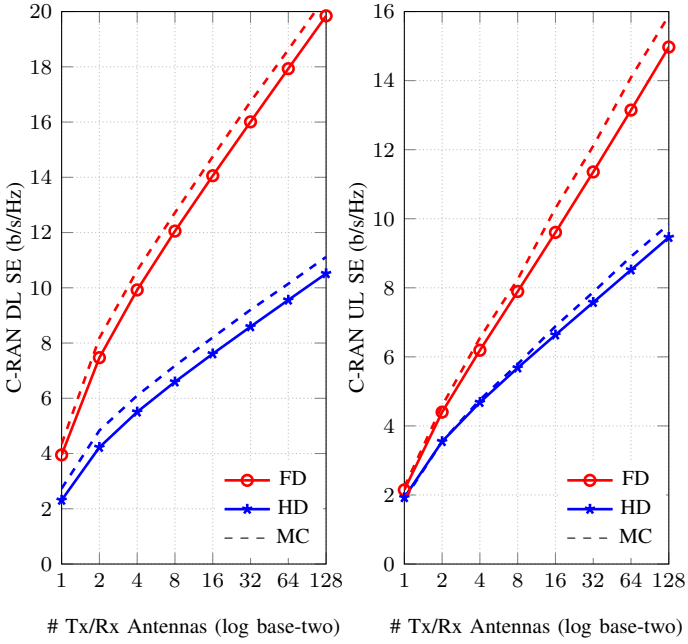

Fig. 2: $L = 3$, $\mathcal{K}^{(d)} = \mathcal{K}^{(u)} = 1$.

REFERENCES

[1] H. Guan, T. Kolding, and P. Merz, "Discovery of Cloud-RAN," 2010.

[2] China Mobile, "C-RAN: the road towards green RAN," *White Paper*, 2011.

[3] T. Quek, M. Peng, O. Simeone, and W. Yu, *Cloud Radio Access Networks: Principles, Technologies, and Applications*. Cambridge University Press, 2017.

[4] A. Checko, H. L. Christiansen, Y. Yan, L. Scolari, G. Kardaras, M. S. Berger, and L. Dittmann, "Cloud RAN for mobile networks – a technology overview," *IEEE Commun. Surveys Tuts.*, vol. 17, no. 1, pp. 405–426, First Quart. 2015.

[5] M. Peng, C. Wang, V. Lau, and H. V. Poor, "Fronthaul-constrained cloud radio access networks: insights and challenges," *IEEE Trans. Wireless Commun.*, vol. 22, no. 2, pp. 152–160, Apr. 2015.

[6] S. Goyal, P. Liu, S. S. Panwar, R. A. Difazio, R. Yang, and E. Bala, "Full duplex cellular systems: will doubling interference prevent doubling capacity?" *IEEE Commun. Mag.*, vol. 53, no. 5, pp. 121–127, May 2015.

[7] T. Riihonen, S. Werner, and R. Wichman, "Mitigation of loopback self-interference in full-duplex MIMO relays," *IEEE Trans. Signal Process.*, vol. 59, no. 12, pp. 5983–5993, Dec. 2011.

[8] M. Duarte, C. Dick, and A. Sabharwal, "Experiment-driven characterization of full-duplex wireless systems," *IEEE Trans. Wireless Commun.*, vol. 11, no. 12, pp. 4296–4307, Dec. 2012.

[9] C. Psomas, M. Mohammadi, I. Krikidis, and H. A. Suraweera, "Impact of directionality on interference mitigation in full-duplex cellular networks," *IEEE Trans. Wireless Commun.*, vol. 16, no. 1, pp. 487–502, Jan. 2017.

[10] A. Shojaeifard, K.-K. Wong, M. D. Renzo, G. Zheng, K. A. Hamdi, and J. Tang, "Massive MIMO-enabled full-duplex cellular networks," *IEEE Trans. Commun.*, accepted 2017.

[11] I. Atzeni and M. Kountouris, "Full-duplex MIMO small-cell networks with interference cancellation," *ArXiv e-prints*, 2016.

[12] O. Simeone, E. Erkip, and S. Shamai, "Full-duplex cloud radio access networks: An information-theoretic viewpoint," *IEEE Wireless Commun. Lett.*, vol. 3, no. 4, pp. 413–416, Aug. 2014.

[13] M. A. A. Khojastepour, K. Sundaresan, S. Rangarajan, and M. Farajzadeh-Tehrani, "Scaling wireless full-duplex in multi-cell networks," in *Proc. IEEE Conf. Comput. Commun. (INFOCOM)*, Apr. 2015, pp. 1751–1759.

[14] M. Mohammadi, H. A. Suraweera, and C. Tellambura, "Full-duplex Cloud-RAN with uplink/downlink remote radio head association," *ArXiv e-prints*, 2016.

[15] A. Shojaeifard, K. K. Wong, M. D. Renzo, G. Zheng, K. A. Hamdi, and J. Tang, "Self-interference in full-duplex multi-user MIMO channels," *IEEE Commun. Lett.*, vol. 21, no. 4, pp. 841–844, Apr. 2017.

[16] K. Hosseini, W. Yu, and R. S. Adve, "A stochastic analysis of network MIMO systems," *IEEE Trans. Signal Process.*, vol. 64, no. 16, pp. 4113–4126, Aug. 2016.

[17] T. M. Cover and J. A. Thomas, *Elements of Information Theory*. Wiley-Interscience, 1991.

[18] M. D. Renzo and P. Guan, "Stochastic geometry modeling of coverage and rate of cellular networks using the Gil-Pelaez inversion theorem," *IEEE Commun. Lett.*, vol. 18, no. 9, pp. 1575–1578, Sept. 2014.